



# Bulletin of the Mineral Research and Exploration

<http://bulletin.mta.gov.tr>



## GEOCHEMICAL CHARACTERISTICS OF LATERITES: THE AILIBALTALU DEPOSIT, IRAN

Ali ABEDINI<sup>a</sup>, Ali Asghar CALAGARI<sup>b</sup>, Khadijeh MIKAEILI<sup>b</sup>

<sup>a</sup> Department of Geology, Faculty of Sciences, University of Urmia, 57153165, Urmia, Iran

<sup>b</sup> Department of Geology, Faculty of Natural Sciences, University of Tabriz, 5166616471, Tabriz, Iran

### Keywords:

Laterite, Protolith,  
Elemental distribution,  
Alibaltalu, Shahindezh,  
Iran

### ABSTRACT

Alibaltalu laterite deposit is located ~20 km northeast of Shahindezh, south of West-Azarbaidjan province (NW of Iran). This deposit is developed as stratiform lenses along the boundary of Elika dolomites (Triassic) and Shemshak sandstones (Jurassic). The distribution fashion of minerals such as boehmite, diaspore, kaolinite, muscovite-illite, rutile, anatase, hematite and goethite in this deposit was accompanied by the development of four types of ore facies: (1) ferrite; (2) laterite; (3) bauxitic kaolinite; and (4) kaolinitic bauxite. Petrographically, the ores show conglomeratic, rounded-granular, veinlet, colloform, pelitomorph, pseudo-porphyratic, nodular, and spongy textures. Comparison of distribution pattern of elements along a selective profile across the deposit reveals that ferruginization-deferruginization mechanism played a prominent role in distribution of Al, Si, Ti, HFSE, LREEs, HREEs, U, and Th during weathering processes. Distribution pattern of REEs normalized to chondrite indicates a poor differentiation of LREEs from HREEs and generation of poor negative Eu anomaly during the evolution of this deposit. These aspects along with ratios of  $Al_2O_3/TiO_2$  and intense differentiation of Al from Fe in the course of weathering processes may indicate a mafic protolith for the deposit. Geochemical consideration of low-mobile elements demonstrates that this deposit is likely resulted from alteration and weathering of basaltic to andesitic rocks. By regarding to the distribution mode of elements such as Ni, Cr, Zr, and Ga within the ores, it can be deduced that this deposit was initially formed authigenically and then later was contaminated by other rock materials during erosion and transportation from its original place to the present site.

## 1. Introduction

Laterites are an important source of many metal ores, in particular iron, aluminium, nickel, gold, niobium, and phosphorus (Hill et al., 2000; Retallack, 2010). The controls necessary for the enrichment of these and other elements to achieve economic levels are a complex balance of geochemical, geographical, and biological parameters (Hill et al., 2000). Specific conditions leading to laterite formation have been documented previously (Bardossy and Aleva, 1990; Ma et al., 2007; Sanematsu et al., 2011). During past two decades lateritic deposits in different parts of the world were studied in detail for realization of factors related to mobilization and redistribution of major, minor, and trace elements (including REE) during

weathering processes (Ma et al., 2007; Yang et al., 2008; Hao et al., 2010; Meshram and Randive, 2011; Sanematsu et al., 2011). These studies revealed that consideration of major and trace elements geochemistry is an indispensable tool to investigate various aspects of laterite formation such as parent rock composition, diagenetic and epigenetic processes related to lateritization, pH, Eh, drainage, climate, and mineralogical control.

Laterite deposits in Iran are apatially distributed in four regions, namely (1) the northwest of Iran, (2) the Zagros heights, (3) the Alborz mountain chain and (4) the central plateau of Iran (Calagari and Abedini, 2007; Abedini and Calagari, 2013a, b). They are restricted to Permian, Permo-Triassic, Triassic,

\* Corresponding author : [abedini2020@yahoo.com](mailto:abedini2020@yahoo.com) and [a.abedini@urmia.ac.ir](mailto:a.abedini@urmia.ac.ir)

Triassic-Jurassic, middle Cretaceous (Cenomanian-Turonian). In northwest of Iran, there are many lateritic deposits belonging mainly to Permian, Permo-Triassic, Triassic, and Triassic-Jurassic period. They chiefly were developed within carbonate rocks and often contain bauxite and kaolinite ores. No comprehensive studies has been done so far on factors influencing distribution of elements in Triassic-Jurassic ores of this type of deposits in northwest of Iran. In this study, Alibaltalu laterite deposit (located in 20 km northeast of Shahindezh, south of West-Azarbaidjan province, NW Iran) as a typical example of this type of deposits was chosen and textural and genetic characteristics, the mineralogical control on distribution of elements (especially trace and rare earth), and ultimately the protolith of this deposit were considered in detail.

## 2. Regional Geology

Based on depositional characteristics of residual deposits throughout the world (Bardossy, 1982) the lateritic deposit of Alibaltalu is reckoned to be a part of Irano-Himalayan karst bauxite belt. This deposit is part of the Sanandaj-Sirjan structural zone (Figure 1a). The palaeogeography of Iran in the Late Permian and Early Triassic indicates that the early Late Triassic compression phase (early Cimmerian event) was followed by extensional movements in north and central Iran (Esmaily et al., 2010). The initiation of this extensional phase is locally indicated by continental alkali-rift basaltic lava flows and vesicular mafic rocks (Berberian and King, 1981; Vollmer, 1987). In Iran, the Late Triassic andesitic to basaltic volcanic rocks cover an eroded and often karstified surface of Middle Triassic carbonates (Early Cimmerian palaeorelief), at the base of the Shemshak Formation (lower Jurassic) (Annelles et al., 1975). The volcanic activity occasionally continued into the lower part of the Shemshak Formation. Some of these basic sources, however, due to laterization processes were partially converted into laterite.

## 3. Method of Investigation

Studies of lateritic ores in study area were carried out in two parts, (1) field and (2) laboratory. The field works include surveys for exploring the existing geological formations, determining the geometry of deposit, examining the lithology of bedrocks, cap rocks, and mesoscopic characteristics of the ores on outcrops, taking random and systematic samples from ores (preferentially perpendicular to the strike of

layers and enclosing rocks), and finally preparing geological map of the area (Figure 1). By noting the lithologic variations in the area, ~40 samples from lateritic ores, bed rocks, and cap rocks were taken for close examination.

Laboratory works include identification of the existing ore textures and their mineralogical compositions. Laboratory studies began after preparation of 20 thin-polished sections and subsequently they were examined microscopically for the existing textures. The mineralogical composition of Six samples were determined by using X-ray diffraction (SIEMENS Diffractometer, Model D-5000, CuK $\alpha$  radiation, fixed graphite chromators, voltage 40kV, current 40 mA, Scanning speed per minute, scan range 2-70°, drive axis 2  $\Theta$ ) in Geological Survey of Iran. For geochemical interpretation 6 samples from lateritic ores were chemically analyzed by ICP-AES and ICP-MS methods at ALS Chemex laboratories in Canada. Loss on ignition (LOI) derives by weight difference after ignition at 1000°C. The results of chemical analyses along with detection limits are listed in table 1.

## 4. Results

### 4.1. Geology of Deposit

The most conspicuous rock units in the study area from the oldest to the youngest include formations such as Mila cherty dolomite and limestone (Cambro-Ordovician), Dorud sandstone and shale (lower Permian), Ruteh carbonate (upper Permian), Elika limestone and dolomite (Triassic), Shemshak sandstone, shale, and siltstone (lower Jurassic), sandy and marly limestone (upper Cretaceous), Fajan conglomerate (Eocene), and Karaj tuff and shale (Eocene) (Figure 1b). There are also a series of basaltic-andesitic rocks occurring as irregular patches within the upper part of Triassic carbonates. The prominent feature from economic geology point of view in the area is the presence of a horizon of stratiform and lenticular lateritic ores along the boundary of Elika dolomite and Shemshak sandstone. This horizon extends about 400 meters and its average strike and dip are N15°W and 83°SW, respectively, with thicknesses ranging from 8 to 14 meters. A selective profile across this horizon exhibits six colored lithologic units including (1) violet-gray, (2) chocolate brown, (3) red, (4) multi-color, (5) yellow, and (6) brown (Figure 2). The boundaries between lateritic lenses and the enclosing

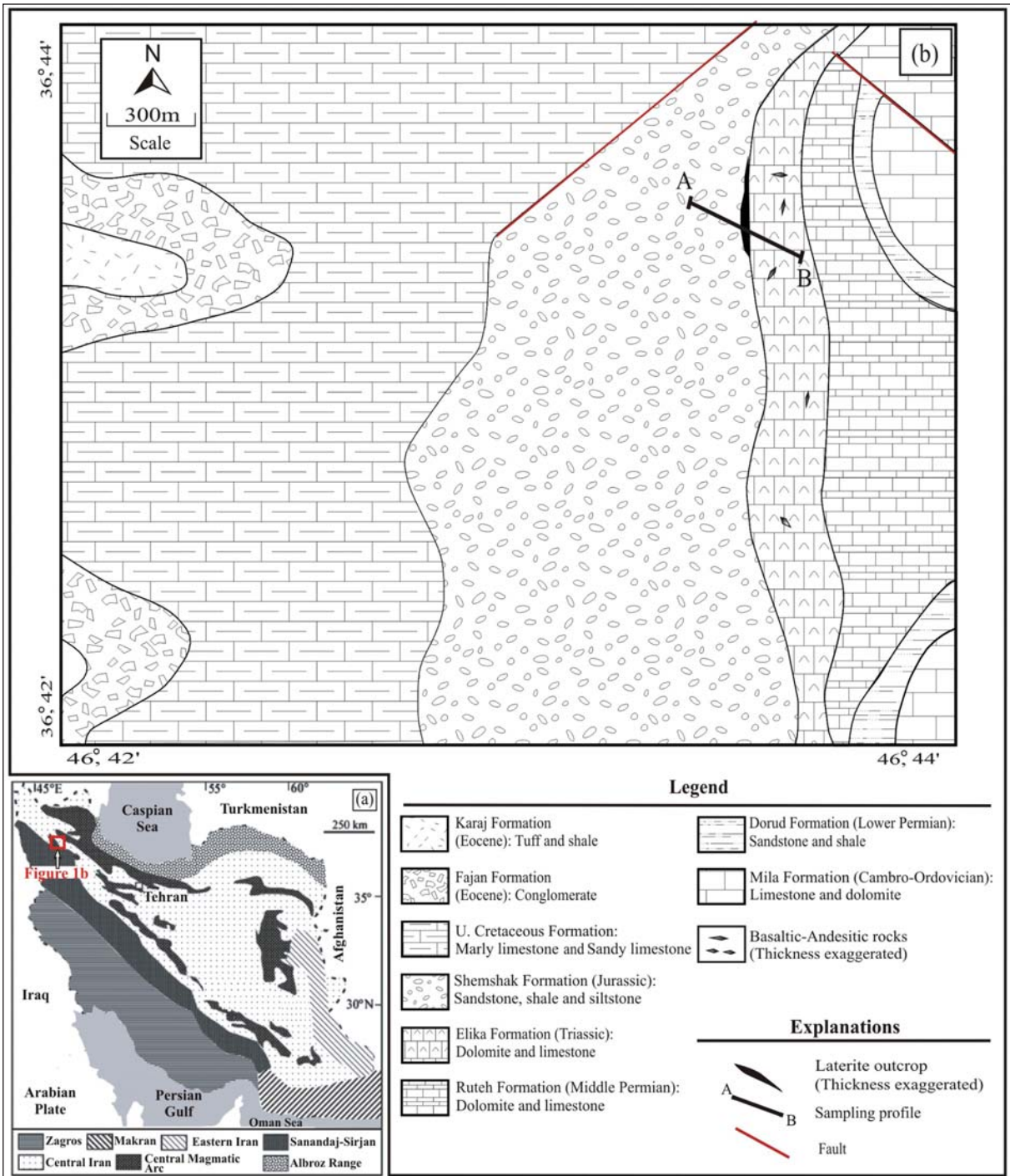


Figure 1- (a) Simplified regional geotectonic map of Iran showing some major geological-structural zones. Location of studied area is also marked (modified after Stöcklin, 1968). (b) Geologic map of the Alibaltalu area. Noticeable on this map is the position of lateritic lens.

bedrocks and cap rocks are quite sharp. There are cross-cutting fractures and joints within the enclosing rocks. Some volcanic rocks are present at contiguity of ore-bedrock boundary. The presence of organic matters in upper parts of the profile is also noticeable. The violet-gray ores have massive texture, fine

alternate violet and gray layers, spheroidal bands consisting of limonite, goethite, and hematite (Figure 3a), delicate porous ring bands with limonitic nucleus (Figure 3b), rough feel, and rather high hardness. On the other hand, however, the chocolate brown ores are rather soft and have earthy aggregates. On the surface

Geochemical Characteristics of Laterites: The Ailibaltalu Deposit, Iran

Table 1- List of chemical analyses in ores of the studied profile done by ICP-AES and ICP-MS methods for major, minor, trace, and rare earth elements. Shown on this table are also are the detection limits of various elements. Values of oxides and L.O.I. are in wt% and of trace and rare earth elements are in ppm.

	Detection limit	R-1	R-2	R-3	R-4	R-5	R-6
SiO <sub>2</sub>	0.01	28.2	5.1	31	4.7	39.5	32.1
Al <sub>2</sub> O <sub>3</sub>	0.01	17.1	2.8	27.6	2.2	33.2	33.6
Fe <sub>2</sub> O <sub>3</sub>	0.01	35.1	78.9	21.6	81.8	8.37	7.21
CaO	0.01	0.28	0.14	0.08	0.26	0.24	0.41
MgO	0.01	0.89	0.19	0.06	0.18	0.12	0.38
Na <sub>2</sub> O	0.01	0.1	0.05	0.06	0.16	0.2	0.06
K <sub>2</sub> O	0.01	2.82	0.45	0.05	0.27	0.08	0.9
TiO <sub>2</sub>	0.01	1.78	0.22	4.5	0.11	4.89	4.33
MnO	0.01	0.43	1.53	0.02	1.36	0.01	0.06
P <sub>2</sub> O <sub>5</sub>	0.01	0.17	0.15	0.59	0.04	0.14	0.36
LOI	0.01	11.75	10.35	12.05	9.41	14.35	20.3
Total	–	98.62	99.88	97.61	100.49	101.1	99.71
U	0.05	6.81	1.53	13.35	1.78	15.2	18.65
V	5	85	5	281	5	358	367
Y	0.5	50.7	9.6	34.1	15.5	30.2	39.7
Zn	5	80	54	46	91	82	73
Zr	2	224	21	434	14	496	525
Ba	0.5	337	168.5	184	87.4	125.5	236
Co	0.5	27.4	21.9	3.3	19.8	6.6	18.8
Cr	10	50	10	80	20	120	180
Cs	0.01	13.9	1.29	0.28	0.84	0.37	1.97
Ga	0.1	25.6	4	31.7	3.8	40.4	46.6
Hf	0.2	5.9	0.5	10.7	0.3	12.3	13.1
Nb	0.2	32.6	1.6	75	0.6	101	116
Ni	5	15	5	31	5	34	79
Pb	5	66	17	38	7	49	32
Rb	0.2	112.5	16	2.7	11.3	3	24.7
Sr	0.1	280	171	3780	125.5	414	2280
Ta	0.1	1.9	0.1	4	0.1	5.6	7.1
Th	0.05	14	2.42	13.7	1.48	16.2	23
La	0.5	79.7	9.3	81.2	4.9	77.8	129
Ce	0.5	136	19.1	165.5	11	144.5	252
Pr	0.03	20.7	2.13	19.15	1.31	17.8	24.5
Nd	0.1	88.1	8.8	76.5	6.4	70.9	87.3
Sm	0.03	20.2	1.92	15.6	1.98	13	16.7
Eu	0.03	5.31	0.42	4.23	0.54	3.38	4.66
Gd	0.05	17.2	2	13.9	2.56	11.8	17.25
Tb	0.01	2.38	0.25	1.84	0.4	1.57	2.41
Dy	0.05	12.8	1.68	9.36	2.49	7.95	12.75
Ho	0.01	2.27	0.28	1.63	0.44	1.41	2.18
Er	0.03	6.69	0.85	4.39	1.33	3.82	5.92
Tm	0.01	0.81	0.02	0.47	0.05	0.45	0.83
Yb	0.03	6.19	0.79	3.92	1.16	3.03	5.73
Lu	0.01	0.83	0.07	0.47	0.12	0.4	0.8

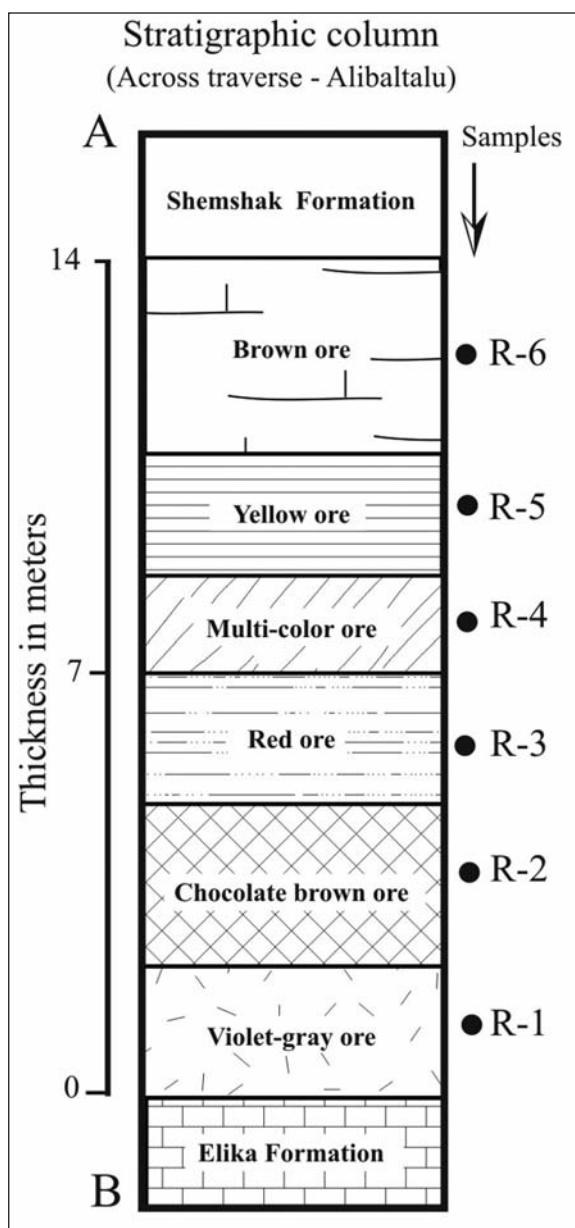


Figure 2- A stratigraphic column across the studied profile. Shown on this column is the location of samples taken for geochemical analyses (filled circles). Refer to figure 1 for the trend of sampling profile.

of the red ores, growth of goethite with a typical botryoidal texture and accompanying limonitization are conspicuous. In fact, these are the important geologic characteristics of the ores in this deposit.

#### 4.2. Petrography and Mineralogy

Because of very fine-grained crystals in ores and their softness, their microscopic examinations are

restricted chiefly to determination of mineral textures related to ore genesis. These studies exhibit that the marked texture-forming units of the ores include pelitomorphic matrix, detrital grains, nodules, concretions, and open-space fillers. These texture-forming units in the ores brought about nodular, pelitomorphic, conglomeratic (Figure 3c), colloform (Figure 3d), pseudo-porphyrific (Figure 3e), veinlet (Figure 3f), rounded-grain (Figure 3g), and spongy (Figure 3h) textures. XRD analyses demonstrate that the ores have rather simple mineralogy and include mineral assemblages like boehmite, diaspore, kaolinite, muscovite-illite, rutile, anatase, hematite, and goethite which have individually abundances greater than 4%.

#### 4.3. Geochemistry

Chemical analyses demonstrate that the major components of the studied ores are  $\text{SiO}_2$  (4.70-39.50 wt%),  $\text{Al}_2\text{O}_3$  (2.20-33.6 wt%),  $\text{Fe}_2\text{O}_3$  (7.21-81.80 wt%), and  $\text{TiO}_2$  (0.11-4.89 wt%) (Table 1). They mark a wide range of variations. Among these components,  $\text{Fe}_2\text{O}_3$  exhibits a profound variation within the profile. Alkalis and earth alkalis along with P and Mn (in oxide form) are present in very low abundance and their total values range from 0.79 to 4.69 wt%.

Trace elements are present relatively in low quantity in the studied ores. They are, in order of abundance, mainly Sr (125.5-3780 ppm), Zr (21-525 ppm), Ba (87.4-337 ppm), V (5-358 ppm), and Ce (11-252 ppm). The rest exist relatively in lower amounts which, in decreasing abundance, are La, Cr, and Zn (in 10s ppm); Th, Rb, Pb, Ni, Nb, Hf, Ga, Cs, Co, Y, V, U, Dy, Gd, Sm, Nd, and Pr (in a few ppm to 10s ppm); and Ta, Eu, Tb, Ho, Er, Tm, Yb, and Lu (in a few ppm).

### 5. Discussion

#### 5.1. Genetic Implications of The Deposit Using Textural and Mineralogical Evidence

##### 5.1.1. Textural Evidence

Important textural characteristics of the studied ores are the existence of two groups of textures with contrasting origin. Pseudo-porphyrific, nodular, and pelitomorphic textures are compatible with authigenic origin whereas conglomeratic and rounded-grain textures are indicative of allogenic origin (Bardossy,

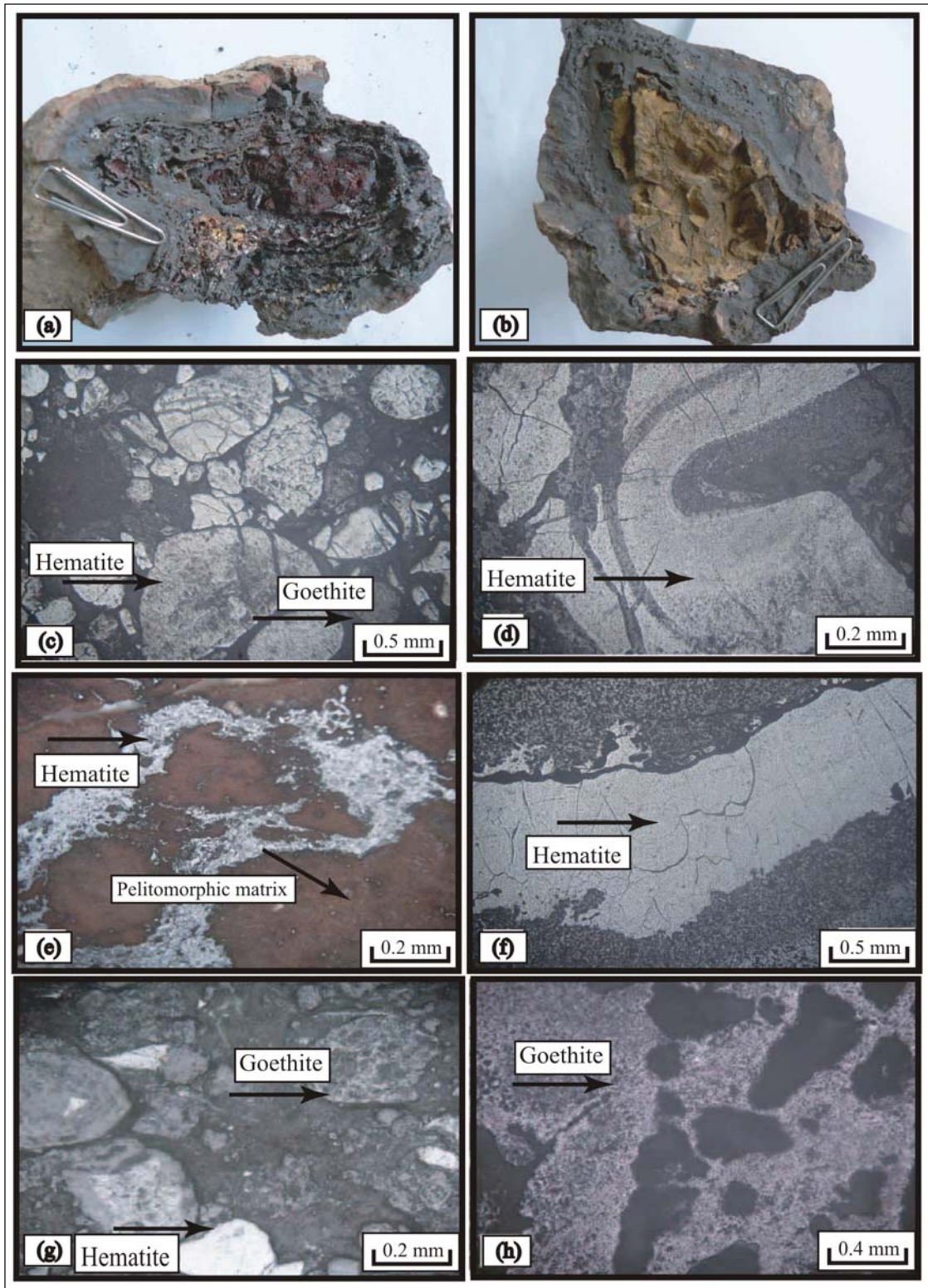


Figure 3- Macroscopic and microscopic (XPL) photographs of the studied ores. (a) Spheroidal weathering and delicate ring bands in porous violet-gray ores. (b) Limonitic core in violet-gray ores. (c) Conglomeratic texture. (d) Colloform texture. (e) Pseudo-porphyrific texture. (f) Veinlet texture. (g) Rounded-grain texture. (h) Spongy texture.

1982). By taking this matter into consideration, it appears that lateritic system in this area was initially developed authigenically but subsequently suffered erosion and transportation and moved to its present place. The development of nodular texture indicates the continuous fluctuations of underground water table level during the evolution of the deposit (Valeton, 1972). The well-developed colloform and pelitomorph textures are indicative of weak draining and prolonged weathering processes (Boulangé, 1984). The presence of veinlets with dominant hematite mineralogy in the ores may testify to the redistribution of iron in the weathered profile.

5.1.2. Mineralogical Evidence

The presence of 3 pairs of minerals (1) boehmite-diaspore, (2) rutile-anatase, and (3) goethite-hematite in the ores denotes the effective role of diagenetic processes and tectonic stresses controlling the mineralogical changes in this deposit. It seems diaspore was formed as the result of changes in crystal structure of boehmite by tectonic stresses and diagenesis (Temur and Kansun, 2006). Anatase is commonly stable in the presence of low concentration of alkali elements at surficial temperatures (Boulangé and Colin, 1994). It probably changed its crystal class by the function of tectonic forces and diagenetic

processes and was converted into rutile. Goethite was also turned into hematite by dehydration processes.

5.2. Type of Ores

Delineation of values of  $Al_2O_3$ ,  $SiO_2$ , and  $Fe_2O_3$  of the ores in trivariate diagram (Aleva, 1994) displays that Alibaltalu deposit consists of four types of ore lithology (1) laterite, (2) ferrite, (3) bauxitic kaolinite, and (4) kaolinitic bauxite (Figure 4a). Comparison of the studied stratigraphic column with distribution mode of  $Al_2O_3$ ,  $SiO_2$ , and  $Fe_2O_3$  of the ores on the trivariate plot indicates that the violet-gray and red ores have lithologically a laterite composition, the chocolate brown and multi-color ores have a ferrite composition, the yellow ores have a bauxitic kaolinite composition, and the brown ores have a kaolinitic bauxite composition (Figure 4b).

5.3. Mineralogical Control on Distribution of Elements in the Ores

In this study, mineral phases having abundances >4% were identified by XRD analyses. Therefore, it is likely that there might be some mineral phases acting as hosts for trace and rare earth elements that were not identified by XRD analyses.

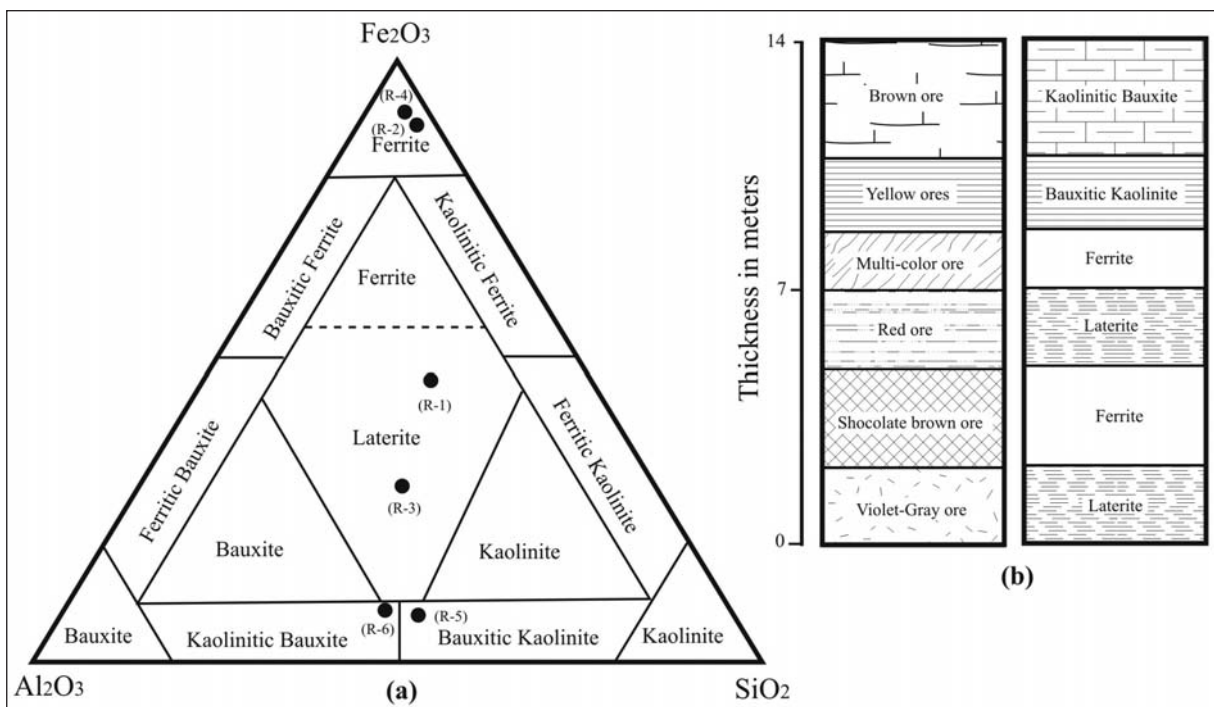


Figure 4- (a) The position of the studied ores on  $Al_2O_3$ - $SiO_2$ - $Fe_2O_3$  trivariate plot (Aleva, 1994). (b) Stratigraphic column of ore units determined by  $Al_2O_3$ ,  $SiO_2$ , and  $Fe_2O_3$  values in the studied profile.

For consideration of minerals hosting elements in the ores, attempts have been made to calculate Pearson correlation coefficient (Rollinson, 1993) among some elements and their distribution patterns were compared (Figure 5-11). This consideration was fulfilled in five sections, (1) major and minor elements (Si, Al, Fe, Ti, K, Na, Mg, Ca, Mn, P), (2) large ion lithophile elements (Ba, Rb, Sr, Th, U, Pb, Cs), (3) transition trace elements (Co, Cr, Ni, V), (4) high field strength elements (Hf, Nb, Ta, Zr, Ga, Y), and (5) light (La-Gd) and heavy (Tb-Lu) rare earth elements.

### 5.3.1. Major and Minor Elements

Similarity in distribution mode of Si (Figure 5a) and Al (Figure 5b) in the residual profile at Alibaltalu

(except yellow to brown ores) shows that the distribution of these elements is controlled principally by kaolinite. Furthermore, the high similarity in distribution mode of Ti (Figure 5c) and Al (Figure 5b) is a common phenomenon in residual profiles. The intense fractionation of Fe (Figure 5d) from Si (Figure 5a), Al (Figure 5b), and Ti (Figure 5c) indicates that ferruginization and deferruginization is the prominent controlling parameter in distribution of Al, Si, and Ti in the profile. What can be deduced from consideration of minor elements variations (Figures 6a-f) is that the irregular behavior of these elements in the profile is likely related to heterogeneity of the protolith and to disparity in the intensity of alteration in the course of evolution of this deposit. Comparison of the mode of variations of minor elements in the profile with that of major

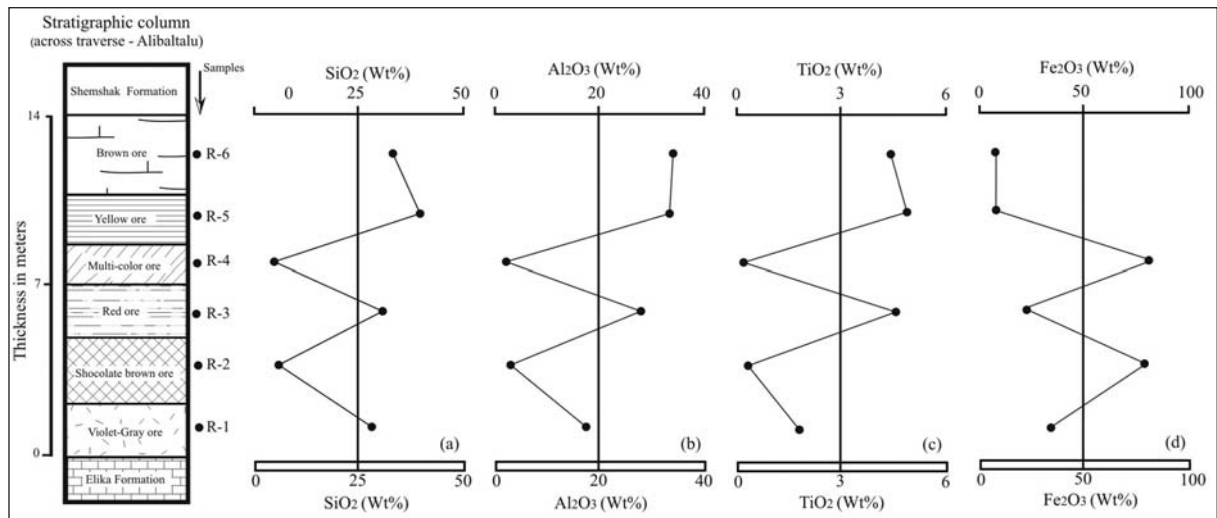


Figure 5- Variation of values of (a) SiO<sub>2</sub>, (b) Al<sub>2</sub>O<sub>3</sub>, (c) TiO<sub>2</sub>, and (d) Fe<sub>2</sub>O<sub>3</sub> across the studied profile.

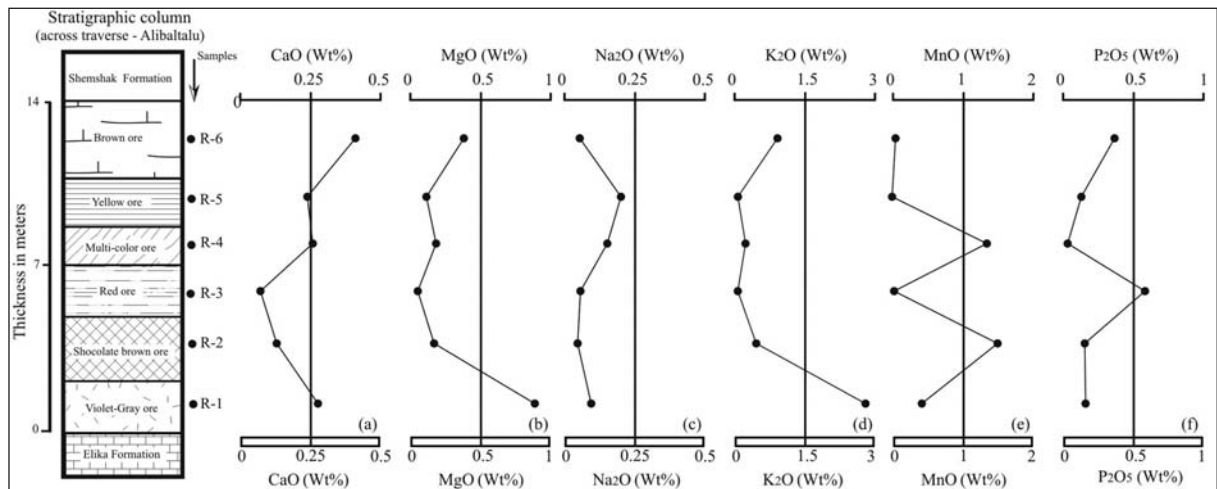


Figure 6- Variation of values of (a) CaO, (b) MgO, (c) Na<sub>2</sub>O, (d) K<sub>2</sub>O, (e) MnO, and (f) P<sub>2</sub>O<sub>5</sub> across the studied profile.

elements illustrates that only Mn (Figure 6e) has very analogous distribution fashion with Fe (Figure 5d). This may indicate that change in redox potential was the key factor in concentration of Mn and Fe in the weathered profile (Ma et al., 2007).

5.3.2. Large Ion Lithophile Elements (LILE)

The presence of similar distribution trends of Rb (Figure 7a), Ba (Figure 7b), and Cs (Figure 7c) with K<sub>2</sub>O (Figure 6d) may be indicative of hosting of these elements by muscovite (Plank and Langmuir, 1998). Comparison between distribution patterns of Sr (Figure 7d) and P (Figure 6f) displays an analogous trend. This may suggest fixation of these elements by similar conditions in the residual system (Henderson, 1984). The positive and medium correlation of Sr with Si (r = 0.55) and Al (r = 0.58) may suggest fixation of Sr by kaolinite. The distribution mode of U (Figure 7e) and Th (Figure 7f) are also similar to Si

(Figure 5a), Al (Figure 5b), and Ti (Figure 5c) suggesting their distributions might have been controlled by kaolinite, boehmite, diaspore and Ti-oxides. Monazite and zircon as Th-bearing minerals are well-known in the residual profiles (Fernandez-Caliani and Cantano, 2010). The similar distribution trend of Th (Figure 7f) and Zr (Figure 8a) and the positive and medium correlation between Th and P (r = 0.52), may suggest that phosphate minerals can also be other candidates for hosting Th. Analogously, the positive and medium correlation between U and P (r = 0.60) may also lead us to believe that phosphate minerals acted as hosts for U. Pb (Figure 7g), Si (Figure. 5a), and Al (Figure 5b) display Similar distributions that may be due to hosting of Pb by kaolinite.

5.3.3. High Field Strength Elements (HFSE)

Consideration of variation mode of these elements in the profile suggests their very similar behavior

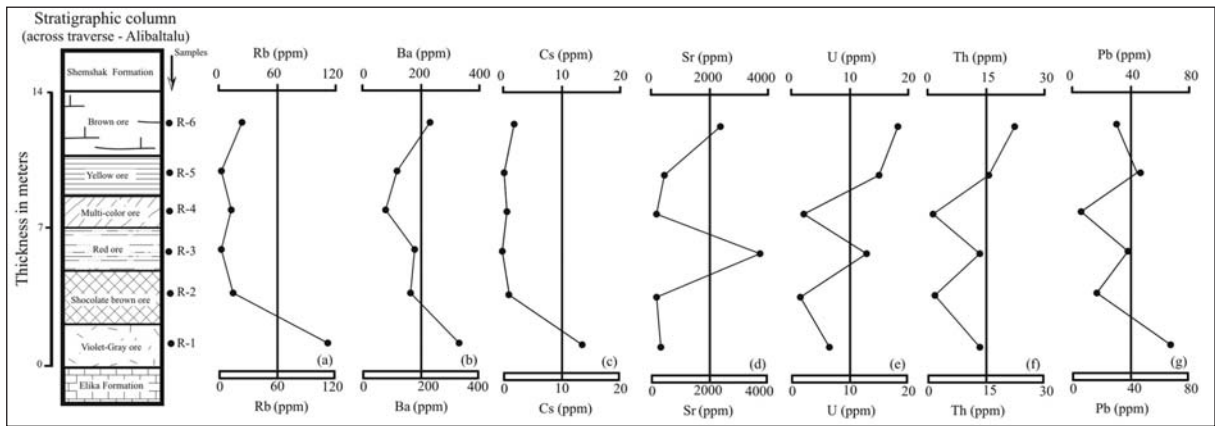


Figure 7- Variation of values of (a) Rb, (b) Ba, (c) Cs, (d) Sr, (e) U, (f) Th, and (g) Pb across the studied profile.

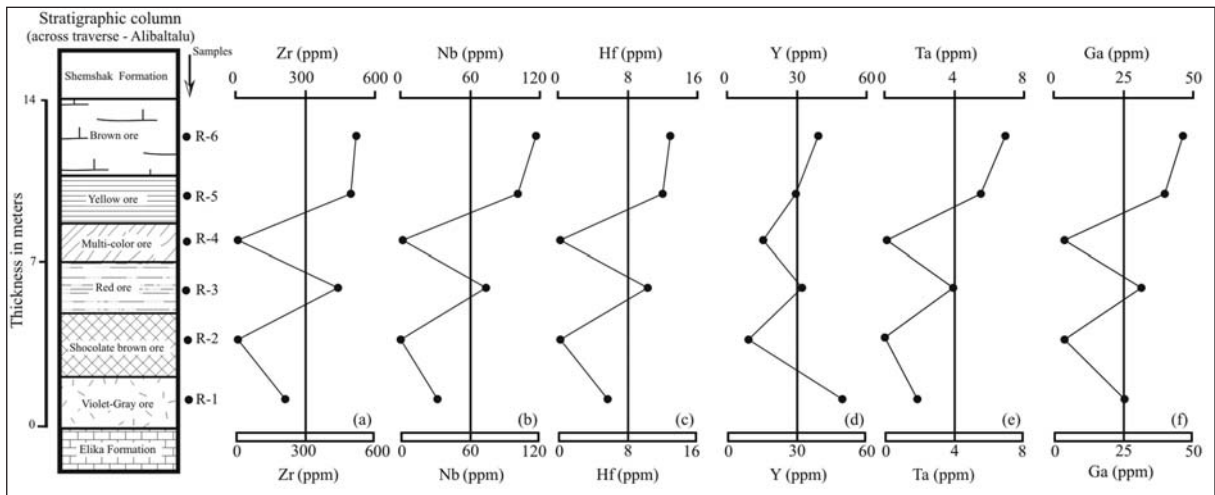


Figure 8- Variation of values of (a) Zr, (b) Nb, (c) Hf, (d) Y, (e) Ta, and (f) Ga across the studied profile.

during weathering processes (Figures 8a-f). Further studies revealed that distribution patterns of these elements are very similar to Al (Figure 5b). Regardless of distribution trend in yellow to brown ores, however, distribution patterns of HFSE are very analogous to Si (Figure 5a) and Ti (Figure 5c). With regard to above mentioned matters, it seems that kaolinite did not play a role for fixation of Y, Ga, Ta, Nb, and Hf in the brown ores, but boehmite and diaspore might have a pronounced role instead. In the rest of ores, however, besides boehmite and diaspore kaolinite also played a noticeable role. Analogous distribution pattern of Zr (Figure 8a), Nb (Figure 8b), Hf (Figure 8c), and Ti, also may suggest that besides mentioned minerals the role of Ti-oxides should not be ruled out for fixation of Zr, Nb, and Hf (Fernandez-Caliani and Cantano, 2010). Ta (Figure 8e) and Ti also exhibit analogous distribution patterns (Figure 5c) implying the notable role of rutile and anatase for fixation of Ta in the deposit.

5.3.4. Transition Trace Elements (TTE)

Although distribution of V, Ni, and Cr in lateritic-bauxitic deposits are chiefly controlled by Fe-oxides and hydroxides (Marques et al., 2004; Laskou and Economou-Eliopoulos, 2007), comparison of their distribution patterns (Figure 9a, b, d) with that of Fe (Figure 5d) do not illustrate such relation in the studied profile. Comparison of distribution patterns of these three elements with those of other major elements manifests that the distribution mode of these

three elements are very much similar to Si (Figure 5a), Al (Figure 5b), and Ti (Figure 5c). These similarities unveil that the distribution of V was controlled by kaolinite, boehmite, diaspore, and Ti-oxides; of Cr by kaolinite and Ti-oxides; and finally of Ni by kaolinite (Newman, 1987). Distribution pattern of Co (Figure 9c) in the yellow through brown ores is analogous to those of V (Figure 9a) and Ni (Figure 9b). Co (Figure 9d), however, in the yellow through violet-gray ores has similar distribution pattern to Fe (Figure 5d) and Mn (Figure 5e). This type of similarity may indicate that the concentration distribution of Co in the brown ores was controlled mainly by kaolinite and Ti-oxides but in the rest of ores by Mn-oxides and Fe-oxides and-hydroxides (Mutakyahwa et al., 2003).

5.3.5. Rare Earth Elements (REEs)

Several groups of minerals were proposed by various researchers as major potential hosts for REEs in weathered products including clays (Karadağ et al., 2009), secondary phosphates (Braun et al., 1993), Mn-oxides and -hydroxides (Walter et al., 1995), and Fe-oxides and -hydroxides (Mameli et al., 2007). Almost similar trends in variation modes exist among LREEs (Figure 10a, b), HREEs (Figures 11a-g), Si (Figure 5a), and Al (Figure 5b) in the studied profile testifying that kaolinite played an outstanding role in distribution of REEs in the ores. The lack of similarity in distribution trends of MnO and F<sub>2</sub>O<sub>3</sub> to those of REEs offers that Mn-oxides along with

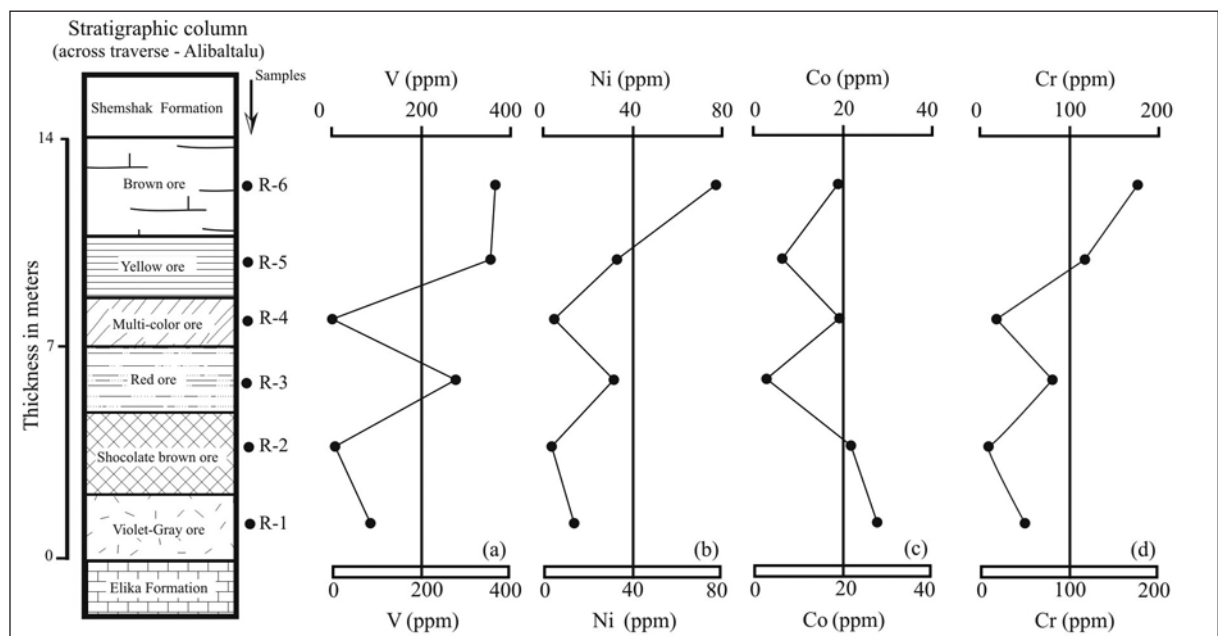


Figure 9- Variation of values of (a) V, (b) Ni, (c) Co, and (d) Cr across the studied profile.

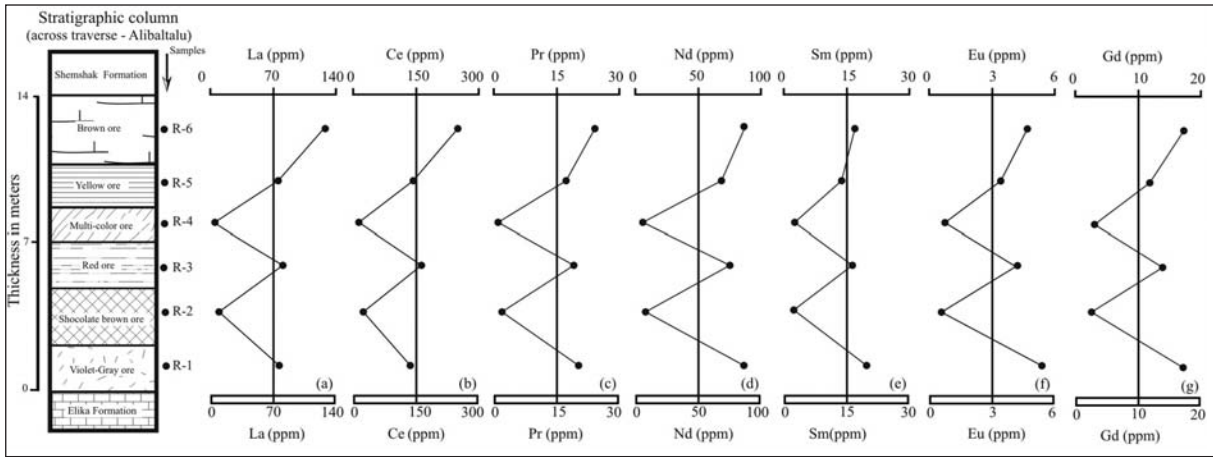


Figure 10- Variation of values of (a) La, (b) Ce, (c) Pr, (d) Nd, (e) Sm, (f) Eu, and (g) Gd across the studied profile.

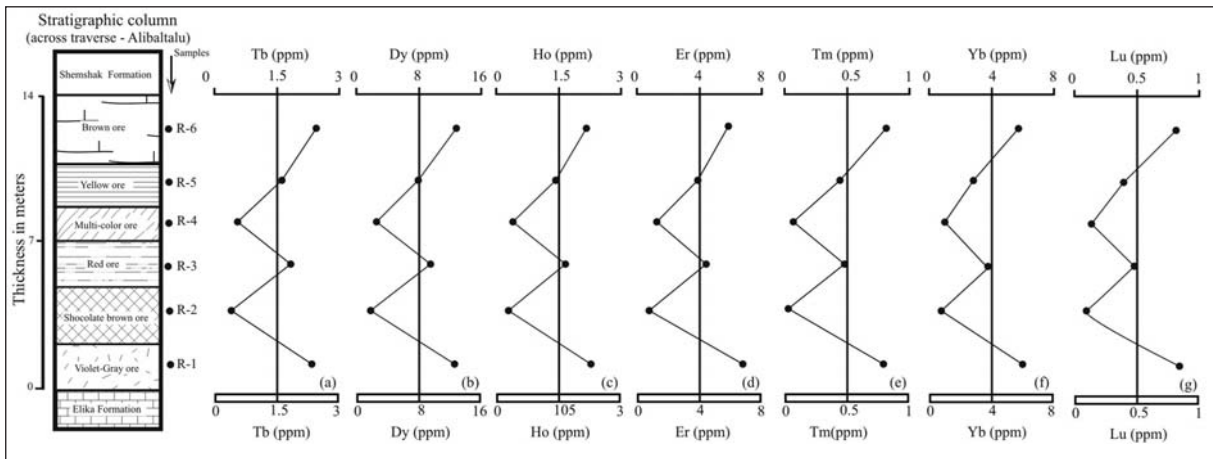


Figure 11- Variation of values of (a) Tb, (b) Dy, (c) Ho, (d) Er, (e) Tm, (f) Yb, and (g) Lu across the studied profile.

hematite and goethite did not have any noticeable role in concentrating of REEs. Although it has not been recognized a specific similarity between K distribution (Figure 6d) and those of REEs (Figures 10a-g, 11a-g), positive and medium correlation between K and HREEs ( $r = 0.52$  to  $0.66$ ) manifests that muscovite-illite may be a potential host for HREEs in the profile. Zircon is reckoned to be chemically the most stable mineral in the course of weathering processes (Oh and Richter, 2005) and could also be a carrier and hence controlling agent for distribution of Ce and HREEs in the weathered system. The similar distribution trends of Zr (Figure 7a), Ce (Figure 10b), and HREEs (Figures 11a-g) could mark the presence of Ce and HREEs in crystal structure of residual zircon (Boulange et al., 1996; Ndjigui et al., 2008). The distribution trends of Ti (Figure 5c) and REEs (Figures 10a-g, 11a-g) to some extent are alike. This is proved by positive and

medium to good correlation between Ti and REEs ( $r = 0.54$  to  $0.85$ ) that may supply strong evidence for the fixation of at least a portion of REEs by rutile and anatase. Phosphorous (Figure 6f) and LREEs (Figure 10a-g) display similar distribution modes particularly in chocolate brown through multi-color units. This could indicate that the distribution of some of the LREEs might be controlled by phosphate minerals in this deposit (Kanazawa and Kamitani, 2006; Roy and Smykatz-Kloss, 2007). HREEs (Figures 11a-g) and Y (Figure 8d) show similar distribution trends. It seems that the Y distribution in the laterite system at Alibaltalu is somehow related to the distribution of HREE. Variation trends of Ce (Figure 10b) and Th (Figure 7f) are also almost alike that may indicate some of Ce and Th in the system were fixed by analogous mechanisms. Similar distribution trends of P (Figure 6b), Al (Figure 5b), and Ce (Figure 10b) in chocolate brown to brown ores along with positive

and medium correlation between Al and P ( $r = 0.58$ ) and positive and good correlation between Al and Ce ( $r = 0.92$ ) may provide enough evidence for the effective role of Al and P-bearing minerals in concentrating some of Ce in the profile.

#### 5.4. Protolith of the Deposit

Several methods were used for determining the protolith of this deposit. Consideration of variation trends of  $Al_2O_3$  (Figure 5b) and  $Fe_2O_3$  (Figure 5d) in the residual profile manifested that intensive separation occurred between Al and Fe during weathering processes. This degree of fractionation commonly takes place between Al and Fe in laterites derived from weathering and alteration of mafic igneous rocks (Schellmann, 1994). Analytic values of  $Al_2O_3$  and  $TiO_2$  of the ores (with assumption that the weathered ores have ratios of  $Al_2O_3/TiO_2 > 21$  for mafic and  $< 21$  for felsic igneous rocks) (Hayashi et al., 1997) were used for determination of potential protolith. These ratios at Alibaltalu range from 6.1 to 20, therefore, it may suggest a mafic origin for the ores. Variation patterns of REEs normalized to chondrite (Taylor and McLennan, 1985) show rather low fractionation of LREEs from HREEs and occurrence of weak Eu anomaly during weathering processes (Figure 12). These aspects could testify to a mafic origin (Nyakairu and Koeberl, 2001).

Using of distribution mode of immobile elements such as Ti, Nb, Zr, and Y in the studied profile is another geochemical method for determination of

protolith. These elements have high potential for being preserved from chemical changes in weathered profiles derived from mafic igneous rocks (Hill et al., 2000; Kurtz et al., 2000). Variation trends of these elements (Figure 8a, b, d, and 5c) are very much the same. By taking the concentration values of these elements into account in the form of  $Nb/Y-Zr/TiO_2$  bivariate plot (Winchester and Floyd, 1977), the protolith of this deposit must have had basaltic, andesitic, and/ or basaltic-andesitic composition (Figure 13). Illustration of Cr and Ni values in a Ni-Cr bivariate plot (Schroll and Sauer, 1968) is another geochemical method being used for determination of the potential protolith. This plot shows that this deposit might have had variable protoliths including basalt, granite, and sandstone (Figure 14). In addition, geochemical data in trivariate plot of Zr-Ga-Cr (Balasubramaniam et al., 1987) reveals that this deposit could have had a wide spectrum of protoliths including mafic and felsic igneous and metamorphic rocks (Figure 15). By referring to above mentioned matters and the allogenic origin of this deposit, it can be further inferred that this deposit was derived initially from alteration and weathering of basaltic to andesitic rocks and subsequently underwent erosion and transportation to its current site where by contamination by other crustal rocks occurred.

#### 6. Conclusions

Alibaltalu residual deposit was developed as stratiform lenses along the contact of Elika dolomite (Triassic) and Shemshak sandstone (lower Jurassic).

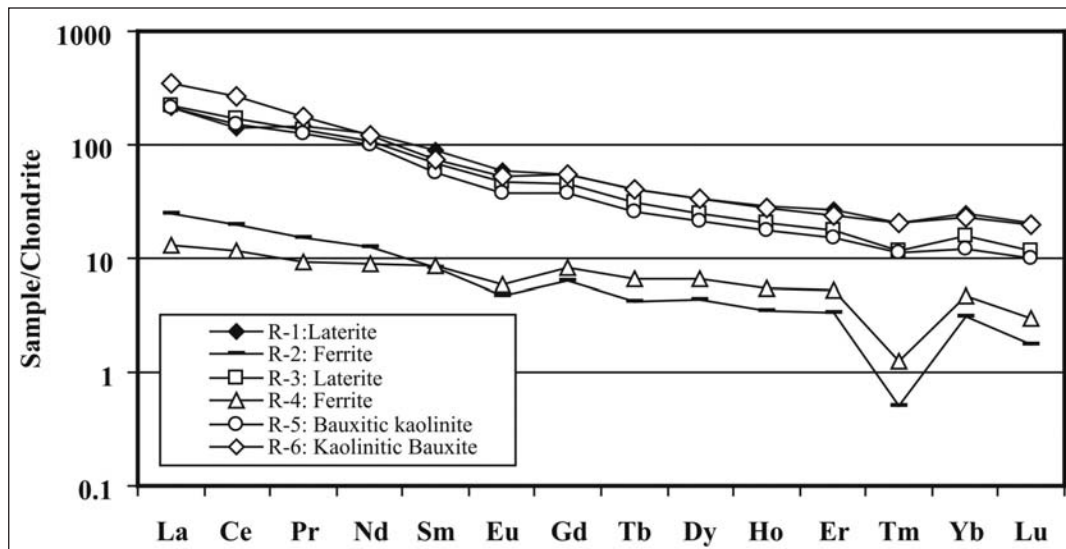


Figure 12- Variation pattern of REEs normalized to chondrite (Taylor and McLennan, 1985) in the studied samples.

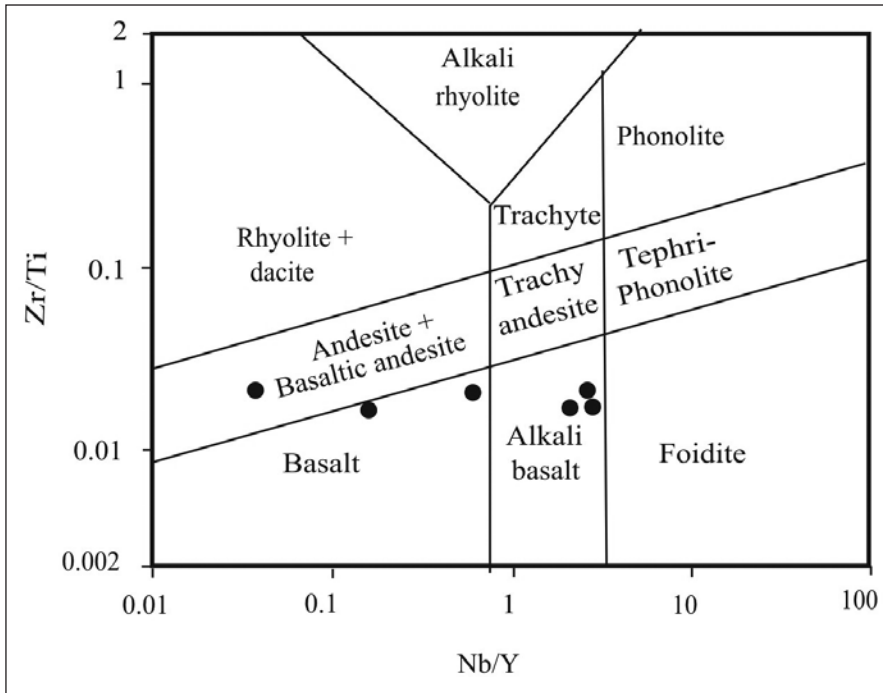


Figure 13- Position of lateritic ores of the studied profile on a bivariate plot of Zr/Ti-Nb/Y (Winchester and Floyd, 1977).

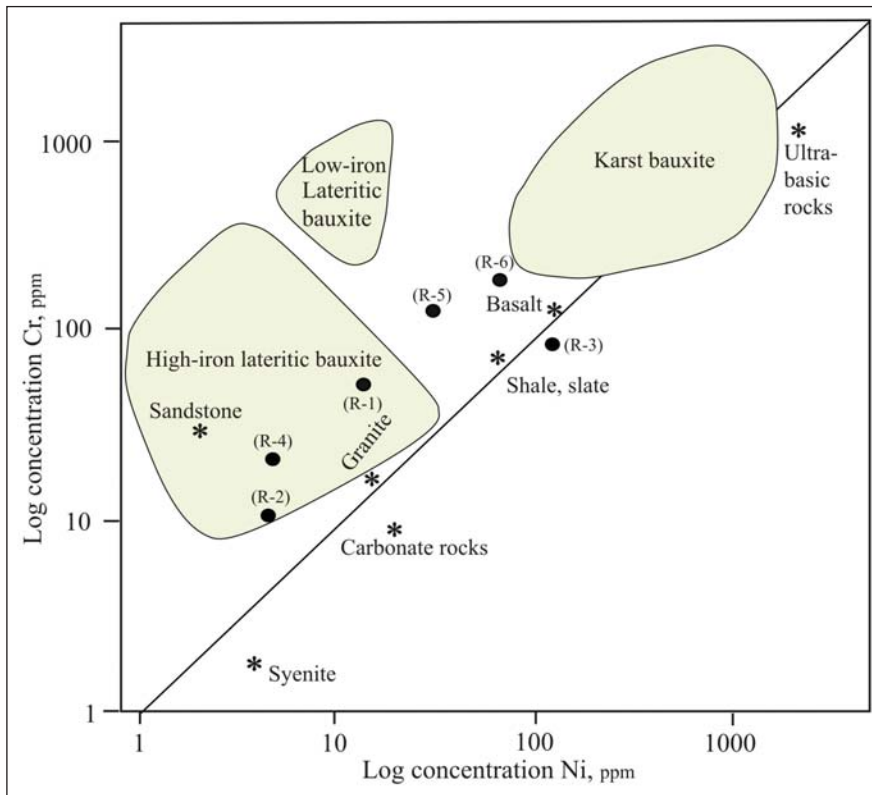


Figure 14- Position of the ores of the studied profile on a bivariate plot of Ni-Cr (Schroll and Sauer, 1968).

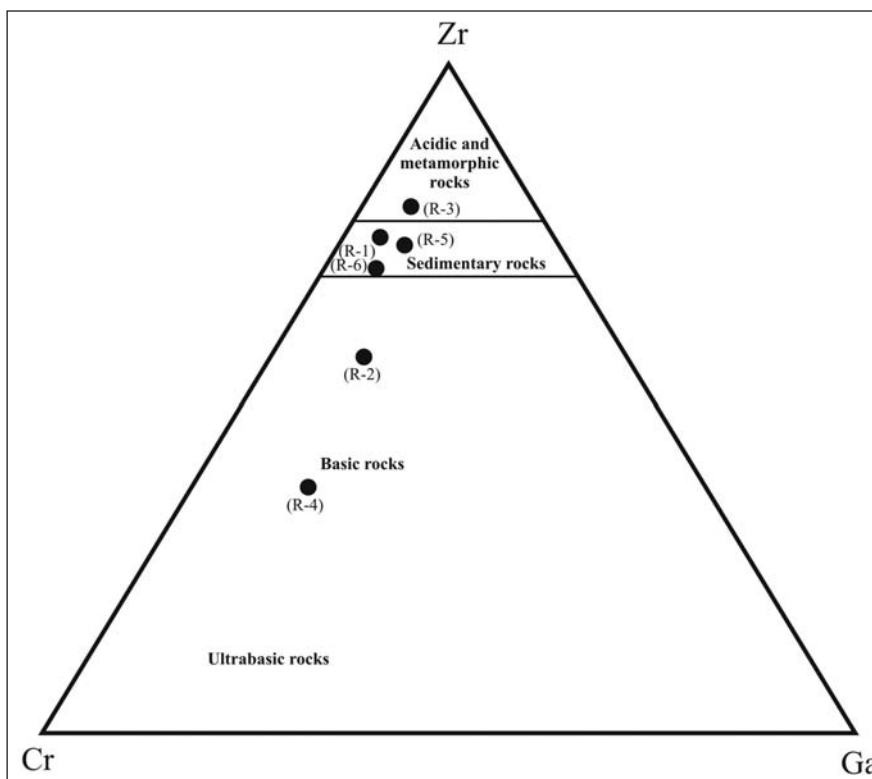


Figure 15- Position of the ores of the studied profile on a trivariate plot of Cr-Ga-Zr (Balasubramaniam et al., 1987).

It consists of four various types of ores including (1) laterite, (2) ferrite, (3) bauxitic kaolinite, and (4) kaolinitic bauxite. By regarding to the presence of conglomeratic and rounded-grain textures, this deposit has an allogenic origin. Rather strong differentiation of Al from Fe during weathering, rather low fractionation of LREEs from HREEs, and weak negative anomaly of Eu along with values of Nb, Zr, Y, Y, and Ti show that protolith of this deposit must have had a composition ranging from basalt to andesite. Consideration of Ni, Cr, Zr, and Ga values in the ores proves that this deposit has an allogenic origin derived from basaltic and andesitic rocks and was subsequently mixed with other terrestrial rock materials during transportation to its current place. Geochemical studies indicate that ferruginization and deferruginization mechanism is the important controlling agent for distribution of Al, Si, Ti, HFSE, LREEs, HREEs, U, and Th in this deposit. Variation patterns of elements show that HFSEs are concentrated by zircon, Ti-oxides, boehmite, diaspore, and kaolinite; TTEs by muscovite, kaolinite, boehmite, diaspore, Mn-oxides, and Fe-oxides and -hydroxides; LILEs by kaolinite, belovite, and Mn-oxides; REEs by muscovite-illite, rutile, and anatase.

### Acknowledgments

This work was supported financially by the Research Bureau of Tabriz University. The authors would like to express their thanks and gratitude to the authorities of this bureau. Our gratitude is further expressed to Prof. Taner ÜNLÜ and two anonymous reviewers for reviewing of the manuscript and making critical comments and valuable suggestions.

*Received: 22.07.2013*

*Accepted: 30.10.2013*

*Published: June 2014*

### References

- Abedini, A., Calagari, A.A. 2013a. Rare earth elements geochemistry of Sheikh-Marut laterite deposit, NW Mahabd, West-Azarbaidjan province, Iran. *Acta Geologica Sinica-English Edition* 87, 176–185.
- Abedini, A., Calagari, A.A. 2013b. Geochemical characteristics of Kanigorgeh ferruginous bauxite horizon, West-Azarbaidjan province, NW Iran. *Periodico di Mineralogia* 82, 1–23.
- Aleva, G.J.J., 1994. Laterites: Concepts, Geology, Morphology and Chemistry. *ISIRC, Wageningen*, 169p.

- Balasubramaniam, K.S., Surendra, M., Kumar, T.V. 1987. Genesis of certain bauxite profiles from India. *Chemical Geology* 60, 227–235.
- Annelles, R.N., Arthurton, R.S., Bazely, R.A., Davies, R.G. 1975. E3-E4 Quadrangle, 1:100 000 scale geological Mmap and explanatory text of Qazvin and Rasht. *Geological Survey of Iran, Tehran*.
- Bardossy, G. 1982. Karst Bauxites. *Elsevier Scientific, Amsterdam*, 441p.
- Bardossy, G.Y., Aleva, G.Y.Y. 1990. Lateritic Bauxites. *Akademia, Kiado Budapest*, 646p.
- Berberian, M., King, G.C.P. 1981. Towards a paleogeography and tectonic evolution of Iran. *Canadian Journal of Earth Sciences* 18, 210–265.
- Boulange, B. 1984. Les formation bauxitiques lateriques de Cote d Ivoire. *Travaux et Documents ORSTOM, Paris* 175, 341p.
- Boulange, B., Colin, F. 1994. Rare earth element mobility during conversion of nepheline syenite into lateritic bauxite at Passa Quatro, Minais Gerais, Brazil. *Applied Geochemistry* 9, 701–711.
- Boulange, B., Bouzat, G., Pouliquen, M. 1996. Mineralogical and geochemical characteristics of two bauxitic profiles, Fria, Guinea republic. *Mineralium Deposita* 31, 432–438.
- Braun, J.J., Pagel, M., Herbillon, A., Rosin, C. 1993. Mobilization and redistribution of REEs and Th in a syenitic lateritic profile: A mass balance study. *Geochimica et Cosmochimica Acta* 57, 4419–4434.
- Calagari, A.A., Abedini, A. 2007. Geochemical investigations on Permo-Triassic bauxite deposit at Kanisheeteh, east of Bukan, Iran. *Journal of Geochemical Exploration* 94, 1–18.
- Esmacily, D., Rahimpour-Binab, H., Esna-Ashari, A., Kananian, A. 2010. Petrography and geochemistry of the Jajarm karst bauxite ore deposit, NE Iran: Implications for source rock material and ore genesis. *Turkish Journal of Earth Science* 19 (2), 267–284.
- Fernandez-Caliani, J.C., Cantano, M. 2010. Intensive kaolinization during a lateritic weathering event in southwest Spain: Mineralogical and geochemical inferences from a relict paleosol. *Catena* 80, 23–33.
- Hao, X., Leung, K., Wang, R., Sun, W., Li, Y. 2010. The geomicrobiology of bauxite deposits. *Geoscience Frontiers* 1, 81–89.
- Hayashi, K., Fujisawa, H., Holland, H.D., Ohmoto, H. 1997. Geochemistry of sedimentary rocks from northeastern Labrador, Canada. *Geochimica et Cosmochimica Acta* 61, 4115–4137.
- Henderson, P. 1984. Rare Earth Element Geochemistry. *Elsevier, Amsterdam*, 510p.
- Hill, I.G., Worden, R.H.G., Meighan, I.G. 2000. Geochemical evolution of a paleolaterite: the interbasaltic formation, northern Ireland. *Chemical Geology* 166, 65–84.
- Kanazawa, Y., Kamitani, M. 2006. Rare earth minerals in the world. *Journal of Alloy Compounds* 408/412, 1339–1343.
- Karadağ, M., Küpeli, S., Arik, F., Ayhan, A., Zedef, V., Doyen, A. 2009. Rare earth element (REE) geochemistry and genetic implications of the Mortas bauxite deposit (Seydisehir/Konya-southern Turkey). *Chemie der Erde- Geochemistry* 69, 143–159.
- Kurtz, A.C., Derry, L.A., Chadwick, O.A. 2000. Refractory element mobility in volcanic soils. *Geology* 28, 683–686.
- Laskou, M., Economou-Eliopoulos, M. 2007. The role of micro-organisms on the mineralogical and geochemical characteristics of the Parnassos-Ghiona bauxite deposits, Greece. *Journal of Geochemical Exploration* 93, 67–77.
- Ma, J., Wei, G., Xu, Y., Long, W., Sun, W. 2007. Mobilization and re-distribution of major and trace elements during extreme weathering of basalt in Hainan Island, south China. *Geochimica et Cosmochimica Acta* 71, 3223–3237.
- Mameli, P., Mongelli, G., Oggiano, G., Dinelli, E. 2007. Geological, geochemical and mineralogical features of some bauxite deposits from Nurra (western Sardinia, Italy): insights on conditions of formation and parental affinity. *International Journal of Earth Sciences* 96, 887–902.
- Marques, J.J., Schulze, D.G., Curi, N., Mertzman, S.A. 2004. Trace element geochemistry in Brazilian Cerrado soils. *Geoderma* 121, 31–43.
- Meshram, R.R., Randive, K.R. 2011. Geochemical study of laterites of the Jamnagar district, Gujarat, India: implications on parent rock, mineralogy and tectonics. *Journal of Asian Earth Sciences* 42, 1271–1287.
- Mutakyahwa, M.K.D., Ikingura, J.R., Mruma, A.H. 2003. Geology and geochemistry of bauxite deposits in Lushoto District, Usambara Mountains, Tanzania. *Journal of African Earth Sciences* 36, 357–369.
- Ndjigui, P., Bilong, P., Bitom, D., Dia, A. 2008. Mobilization and redistribution of major and trace elements in two weathering profiles developed on serpentinites in the Lomie ultramafic complex, southeast Cameroon. *Journal of African Earth Sciences* 50, 305–328.
- Newman, A.D.C. 1987. Chemistry of Clay and Clay Minerals. *Mineralogical Society, Monograph* 6, 480 p.
- Nyakairu, G.W.A., Koeberl, C. 2001. Mineralogical and chemical composition and distribution of rare earth elements in clay rich sediments from Central Uganda. *Geochemical Journal* 35, 13–28.
- Oh, N.H., Richter, D.D. 2005. Elemental translocation and loss from three highly weathered soil- bedrock profiles in the southeastern United States. *Geoderma* 126, 5–25.
- Plank, T., Langmuir, C.H. 1998. The chemical composition of subducting sediment and its consequences for

- the crust and mantle. *Chemical Geology* 145, 325–394.
- Retallack, G.J. 2010. Lateritization and bauxitization events. *Economic Geology* 105, 655–667.
- Rollinson, H. 1993. Using Geochemical Data: Evaluation, Presentation, Interpretation. *Longman Scientific and Technical*, 352p.
- Roy, P.D., Smykatz-Kloss, W. 2007. REE geochemistry of the recent playa sediments from the Thar Desert, India: an implication to playa sediment provenance. *Chemie der Erde- Geochemistry* 67, 55–68.
- Sanematsu, K., Moriyama, T., Sotouky, L., Watanabe, Y. 2011. Mobility of REEs in basalt derived laterite at the Bolaven plateau, Southern Laos. *Resource Geology* 61, 140–158.
- Schellmann, W. 1994. Geochemical differentiation in laterite and bauxite formation. *Catena* 21, 131–143.
- Schroll, E., Sauer, D. 1968. Beitrag zur Geochemie von Titan, Chrom, Nickel, Cobalt, Vanadium und Molybdän in Bauxitischen Gesteinen und problem der stofflichen herkunft des Aluminiums. *Travaux de ICSOBA* 5, 83–96.
- Stöcklin, J. 1968. Structural history and tectonics of Iran, a review. *American Association of Petroleum Geologists Bulletin* 52 (7), 1229–1258.
- Taylor, S.R., McLennan, S.M. 1985. The Continental Crust: Its Composition and Evolution. *Blackwell, Oxford*, 312p.
- Temur, S., Kansun, G. 2006. Geology and petrography of the Masatdagi diasporic bauxites, Alanya, Antalya, Turkey. *Journal of Asian Earth Sciences* 27, 512–522.
- Valeton, I. 1972. Bauxites. *Elsevier*, 226 p.
- Vollmer, T. 1987. Zur Geologie des nordlichen Zentral-Elburz zwischen Chalus- und Haraz-Tal, Iran. *Mitteilungen des Geologisch Paläontologischen Instituts der Universität of Hamburg* 63, 1–125.
- Walter, A.V., Nahon, D., Flicoteaux, R., Girard, J.P., Melfi, A. 1995. Behaviour of major and trace elements and fractionation of REE under tropical weathering of typical weathering of typical apatite-rich carbonatite from Brazil. *Earth and Planetary Science Letters* 303, 591–601.
- Winchester, J.A., Floyd, P.A. 1977. Geochemical discrimination of different magma series and their differentiation products using immobile elements. *Chemical Geology* 20, 325–343.
- Yang, R.D., Wang, W., Zhang, X., Liu, L., Wei, H., Bao, M., Wang, J. 2008. A new type of rare earth elements deposit in weathering crust of Permian basalt in western Guizhou, NW China. *Journal of Rare Earths* 26 (5), 753–758.